ACS POLYMERS Au
AN OPEN ACCESS JOURNAL OF THE AMERICAN CHEMICAL SOCIETY

pubs.acs.org/polymerau
Article

Effects of Polymer Architecture and Charged Molecular Crowders on Hydrophobic Polymer Collapse

Published as part of ACS Polymers Au virtual special issue "Polymer Science and Engineering in India".

Satyendra Rajput and Divya Nayar*

Cite This: *ACS Polym. Au* 2024, 4, 289−301
Read Online

ACCESS | Metrics & More | Article Recommendations

ABSTRACT: Accounting for the crowding effects inside a living cell is crucial to obtain a comprehensive view of the biomolecular processes and designing responsive polymer-based materials for biomedical applications. These effects have long been synonymous with the entropic volume exclusion effects. The role of soft, attractive intermolecular interactions remains elusive. Here, we investigate the effects of model cationic and anionic hydrophobic molecular crowders on the collapse equilibrium of uncharged model polymers using molecular dynamics simulations. Particularly, the effect of polymer architecture is explored where a 50-bead linear polymer model (Poly-I) and a branched polymer model (Poly-II) with nonpolar side chains are examined. The collapse of Poly-I is found to be highly favorable than in Poly-II in neat water. Addition of anionic crowders strengthens hydrophobic collapse in Poly-I, whereas collapse of Poly-II is only slightly favored over that in neat water. The thermodynamic driving forces are quite distinct in water. Collapse of Poly-I is driven by the favorable polymer−solvent entropy change (due to loss of waters to bulk on collapse), whereas collapse of Poly-II is driven by the favorable polymer−solvent energy change (due to favorable intrapolymer energy). The anionic crowders support the entropic mechanism for Poly-I by acting like surfactants, redirecting water dipoles toward themselves, and preferentially adsorbing on the Poly-I surface. In the case of Poly-II, the anionic crowders are loosely bound to polymer side chains, and loss of crowders and waters to the bulk on polymer collapse reduces the entropic penalty, thereby making collapse free energy slightly more favorable than in neat water. The results indicate the discriminating behavior of anionic crowders to strengthen the hydrophobic collapse. It is related to the structuring of water molecules around the termini and the central region of the two polymers. The results address the modulation of hydrophobic hydration by weakly hydrated ionic hydrophobes at crowded concentrations.

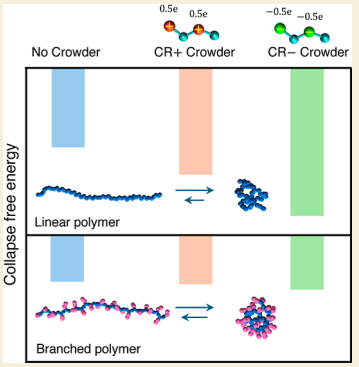

KEYWORDS: *polymer solvation, charged crowders, hydrophobic collapse, molecular simulations, thermodynamics*

INTRODUCTION

Hydrophobic interactions have been known to be crucial for diverse biophysical and chemical phenomena.[1−4] Considerable experimental and theoretical efforts have been devoted over several decades to obtain a molecular view of the hydrophobic effect (or hydrophobic collapse) that drives crucial processes like protein folding and aggregation.[2,5,6] A common consensus, however, is still lacking, and an understanding of the molecular mechanisms remains elusive. Hydrophobic effect arises due to the tendency of nonpolar molecules to self-assemble in order to reduce the exposure of their nonpolar surface to water. An interplay of the direct attraction between the nonpolar solutes and water-mediated interactions is known to determine the strength of the hydrophobic effect.[7] Properties of stimuli-responsive polymer materials, among the other chemical processes, are also known to be guided by the solvation of hydrophobic surfaces and water-mediated interactions.[8] Emerging biomedical applications of these polymer-based smart materials include controlled drug delivery and release systems,[9] smart surfaces for cell adhesion and migration,[10] tissue engineering, and bioseparation.[11]

For such biological functions, these biopolymers require a change in their conformation in response to the change in the environment such as the one that they encounter in the biological fluid or the intracellular environment. In order to probe these effects, therefore, it is necessary to account for the effects exerted by the crowded environment inside a living cell.[12−15] It has been long known that the tight packing (≈20−40% of total volume) of large-sized macromolecules, cosolutes, and ions inside the living cell exert macromolecular crowding effects that drive aggregation or collapse of biomolecules.[16]

Received: February 18, 2024
Revised: April 23, 2024
Accepted: April 24, 2024
Published: May 6, 2024

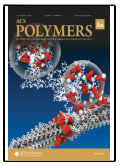

These crowding effects are often associated with the volume exclusion (steric) effects of the crowding macromolecules which are believed to be entropic in origin.[15,17,18] An emerging view suggests that since the intracellular environment also comprises charged cosolutes, ions, and charged macromolecules, it becomes imperative to understand and account for the effects of soft, cohesive intermolecular (enthalpic) interactions on the biomolecular processes.[19−29] Specifically, the effect of a charged molecular crowded environment on the hydrophobic collapse and therefore on the folding−unfolding equilibrium of the biomolecules is relatively less explored.[30]

To understand such effects on hydrophobic collapse, often the coil−globule transition behavior of a hydrophobic polymer is investigated in the aqueous solutions. Understanding the polymer chain collapse has attracted considerable attention partly due to its similarity in exhibiting the two-state conformational scenario as also observed for proteins.[24,31−33] The most popular polymer models have been of the Lennard−Jones homopolymer,[34,35] atomistic or united atom model of polyethylene,[36,37] and atomistic model of polyvinyl chloride[38,39] to examine the collapse behavior in water. All of these studies have primarily examined a linear homopolymer chain in their investigation. However, polymer architecture can play a crucial role in determining the monomer interactions with the other monomers and the solvent, thereby determining the conformational behavior of the polymer. It has been observed that the cosolvents (e.g., urea and trimethylamine *N*-oxide) or osmolytes (e.g., salts) have different propensities to interact with the protein (or polymers like PNIPAM; poly-*N*-isopropylacrylamide) backbone and the side chains that can significantly affect the folding−unfolding equilibrium of proteins.[40−43] Weakly hydrated anions such as SCN^- have been shown to preferentially bind with the amide group of the protein backbone, leading to salting-in or unfolding of the protein.[41] However, the strongly hydrated cations such as Ca^{2+} have been shown to be preferentially depleted from the polymer (PNIPAM) surface, resulting in a decrease in the LCST (promoting salting-out) of the polymer. A recent study by Cremer and co-workers used site-specific NMR spectroscopy to show that the weakly hydrated anions such as SCN^- are excluded from the poly(ethylene oxide) polymer termini but are preferentially bound to the central polymer regions even when the chemical moieties constituting the termini and central regions were identical.[44] They accorded this discriminating preference of the anions to the water structuring around the nonpolar monomers of the polymer. They termed the weakly hydrated anions as "discriminating hydrophobes" that do not bind to all the nonpolar solutes but to those that perturb the water structure considerably. The authors indicated that this could pave way to separate out polymers with identical monomers but different architectures.[44,45]

Therefore, this raises an intriguing question as to how the anionic (and cationic) cosolutes that are at crowded concentrations (or high packing fractions) would affect the collapse of hydrophobic polymers having different architecture? This necessitates including the backbone and side chain features in a simplified polymer model since it not only determines the overall flexibility of the polymer but also would help in determining the role of the chemical details such as of the backbone and the side chains. In this study, we examine the effects of the model small-sized charged cosolutes at crowded packing fractions of 24% (hereafter denoted as *crowders*). These crowders represent monomers of biomolecules such as amino acids and nucleic acids that comprise charged sites. We denote these molecular crowders as *anionic or cationic hydrophobic crowders* since they are weakly charged and have nonpolar groups as well. Several studies have focused only on the *direct* electrostatic interactions of the charged cosolutes or salts with the polar groups in the protein to understand the salting-in or salting-out effects.[43] However, very little is explored about the role of the *indirect* nonspecific weak attractions of the charged cosolutes with the nonpolar groups of the protein or the polymer. Moreover, the hydration of the charged cosolutes, whether weak or strong, is expected to affect the hydration of the polymer which in turn can possibly affect the hydrophobic collapse behavior. We address the following questions: (i) what is the effect of the charged crowded environment on the hydration of an uncharged hydrophobic polymer that can affect its collapse equilibria? (ii) What is the contribution of the polymer backbone versus the nonpolar side chains of the polymer in strengthening or weakening the hydrophobic collapse in the presence of charged crowders? (iii) How does the hydration of charged crowders affect the hydrophobic collapse in the polymers? For this, we compare the polymer collapse equilibrium of the two types of hydrophobic polymers in positively and negatively charged model crowder aqueous solutions: (i) a 50-bead linear polymer (further denoted as Poly-I) and (ii) a branched polymer where two-bead hydrophobic side chains are introduced on a 50-mer backbone (further denoted as Poly-II). The solvation thermodynamics of the polymers in crowded solutions is investigated, and the tendency of the charged crowders to affect the hydrophobic collapse of the two polymers similarly or differently is explored.

METHODS

Solvation Thermodynamics

The hydrophobic polymers examined in this study can be considered to exist in a two-state conformational equilibrium between the collapsed (C) and extended (E) states.[24,33,35,46] The free energy associated with the collapse of the polymer can be written as[32,33]

$$\Delta G^{E\to C} = (\mu_C^* - \mu_E^*) + (\Delta E_{intra}^{E\to C} - T\Delta S_{conf}^{E\to C}) \quad (1)$$

where μ_C^* and μ_E^* are the solvation free energies or the excess chemical potentials of C and E states, respectively. ΔS_{conf} denotes the change in polymer conformational entropy on collapse and ΔE_{intra} is the change in the internal energy of the polymer on collapse due to the intramolecular interactions. The $P\Delta V$ term is negligible at 1 atm.

The microscopic view of solvation can be obtained using the Widom potential distribution theorem that allows one to connect the excess chemical potential of the polymer (μ^*) with the polymer (solute)−solvent intermolecular energy. It is the reversible work done for slowly turning on the solute−solvent interactions when the polymer is inserted into the solvent. Using the inverse form of the Widom potential distribution theorem, it can be expressed as

$$e^{\mu^*/RT} = \langle e^{\phi/RT} \rangle \quad (2)$$

where ϕ is the solute (polymer)−solvent (crowders and water) interaction energy and $\langle \cdots \rangle$ denotes the ensemble average over all the configurations of polymer solution. In terms of the solute−solvent energy (E_{uv}) and entropy (S_{uv}), it can be written as

$$\mu^* = \langle \phi \rangle + RT\ln\langle e^{\delta\phi/RT} \rangle = E_{uv} - TS_{uv} \quad (3)$$

where the average solute−solvent interaction energy is denoted by $E_{uv} \equiv \langle \phi \rangle$ and the average solute−solvent entropy is denoted by $S_{uv} \equiv -R\ln\langle e^{\delta\phi/RT} \rangle$. A more detailed description on these contributions can be found in refs 32 and 33. Using eqs 1 and 3, the polymer collapse free energy can be written as

https://doi.org/10.1021/acspolymersau.4c00011
ACS Polym. Au 2024, 4, 289−301

$$\Delta G^{E\to C} = \Delta E_{uv}^{E\to C} + \Delta E_{intra}^{E\to C} - T(\Delta S_{uv}^{E\to C} + \Delta S_{conf}^{E\to C}) \quad (4)$$

$$\Delta G^{E\to C} = \Delta E_{pv}^{E\to C} - T\Delta S_{pv}^{E\to C} \quad (5)$$

where, $\Delta E_{pv}^{E\to C} = \Delta E_{uv}^{E\to C} + \Delta E_{intra}^{E\to C}$ and $\Delta S_{pv}^{E\to C} = \Delta S_{uv}^{E\to C} + \Delta S_{conf}^{E\to C}$. Here, $\Delta E_{pv}^{E\to C}$ and $\Delta S_{pv}^{E\to C}$ are the change in polymer−solvent energy and entropy, respectively. The contributions arising from the polymer−crowder, polymer−water, and intrapolymer energy, respectively, sum up to the $\Delta E_{pv}^{E\to C} = \Delta E_{pc}^{E\to C} + \Delta E_{pw}^{E\to C} + \Delta E_{pp}^{E\to C}$ (or $\Delta E_{intra}^{E\to C}$). Here, $\Delta E_{px}^{E\to C} = E_{px}^{C} - E_{px}^{E}$, and x can be p, c, w, or v.

System Setup

The two polymers investigated in this work are uncharged polymers that have only weak van der Waals interactions in the solution. The linear 50-mer uncharged model polymer (Poly-I) was constructed from the previously examined 32-mer uncharged polymer model. The bond length and angle parameters have been taken from the study of Zangi et al.[35] The nonbonded dispersion interactions are modeled by the Lennard−Jones (LJ) potential with the size of the bead taken as σ = 0.40 nm and the interaction energy parameter ε = 1.0 kJ mol^{-1}.[35] The second polymer, Poly-II, was constructed using a backbone of 50 uncharged beads and 25 side chains, each with two uncharged beads that are attached to every alternate backbone bead of the polymer. The bond length, bond angle, and LJ potential parameters used were the same as those used for Poly-I. The snapshots are shown in Figure 1. We

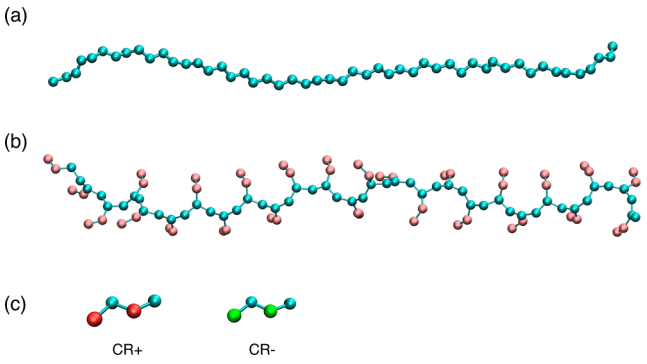

Figure 1. Generic hydrophobic polymers investigated in this study: (a) 50-mer linear Poly-I and (b) branched Poly-II in aqueous crowded solutions of (c) charged hydrophobic tetramer molecules CR+ and CR−.

have employed Lorentz−Berthelot mixing rules to model the unlike interactions. The crowders were modeled as a tetramer of the beads of the Poly-I polymer. A partial charge of +0.5e or −0.5e was introduced on two alternate beads of the crowders, with a sum total charge of either +1e or −1e on the crowder. The positively charged and negatively charged crowders are denoted as CR+ and CR−, respectively. The polymer chain was solvated with water molecules and 330 crowder molecules in a box with cubic periodic boundary conditions. Equal number of counterions were added to neutralize the overall charge of the solution. In case of CR+, Cl^- were added, and Na^+ were added in the solution of CR−. Water was modeled with SPC/E potential. The details of the system composition and size are described in Table 1.

Simulation Details

Molecular dynamics (MD) simulations of the systems were performed using GROMACS-2019.4.[47] The energy of the system was minimized by using the steepest descent algorithm. The systems were equilibrated in an isothermal−isobaric (*NPT*) ensemble for 1 ns (for Poly-I) and 5 ns (for Poly-II) at 300 K and 1 atm pressure, followed by the production run for 10 ns. The temperature and pressure were maintained using the Nose−Hoover thermostat and Parrinello−Rahman barostat, respectively, having the damping coefficient (τ_T =) 1.0 ps and (τ_P =) 2.0 ps, respectively, for both the equilibration and production runs. In all simulations, an integration time step of 2 fs was implemented. A cutoff distance of 1.0 nm was employed to compute the van der Waals interactions, while the electrostatic interactions were computed by using the particle mesh Ewald (PME) method with a grid spacing of 0.12 nm and a real-space cutoff radius of 1 nm. The bond lengths of the solute molecule were constrained by using the LINCS algorithm.

Umbrella Sampling Simulations

To compute the potential of mean force (pmf) profiles, umbrella sampling simulations were conducted using the PLUMED 2.6.0 plugin.[48] It required 60 independent simulations (or windows) using the radius of gyration (R_g) of the polymer as the collective variable. The range of R_g used was 0.40−1.875 nm with a spacing of ΔR_g = 0.025 nm which ensured sufficient overlapping of each window with the adjacent windows for both the polymer systems. Equilibration and production runs were performed in the *NPT* ensemble with the parameters of the thermostat and barostat, as mentioned above. The run lengths for the equilibration were 2 ns and for production runs 10 and 20 ns for Poly-I and Poly-II, respectively. Furthermore, a harmonic bias function, $\omega_i^b(R_g)$, was applied to the R_g of the polymer. And the force constant (strength of the bias) of k_b = 20 000 kJ mol^{-1} nm^{-2} for the harmonic restraint function was applied to be sufficiently large to drive the system over the energy barrier between the C- and E-states of the polymer.

$$\omega_i^b(R_g) = \frac{k_b}{2}(R_g - R_{g,i}^{ref})^2 \quad (6)$$

where $R_{g,i}^{ref}$ is the desired equilibrium value of the reaction coordinate. The unbiased histograms and pmf profiles were obtained over the trajectories using the Weighted Histogram Analysis Method (WHAM).[49] The tolerance value used in the WHAM analysis was taken to be 10^{-5}. The average pmf profile was computed by splitting the trajectory into five blocks, and the standard error was computed from the standard deviation of each block from the total average. The change in free energy on polymer collapse ($\Delta G^{E\to C}$) is calculated using the following equation

$$\exp(-\Delta G^{E\to C}/RT) = \frac{\int_0^{R_g^\#} \exp(-w(R_g)/RT)\mathrm{d}R_g}{\int_{R_g^\#}^{\infty} \exp(-w(R_g)/RT)\mathrm{d}R_g} \quad (7)$$

where R is the gas constant and T is the temperature of the system.

Simulations for Computing Energetics and Observables

In order to compute the polymer−solvent energy contribution to the collapse free energy, large flexible conformational pools of the C- and E-states need to be sampled. For this, separate sets of MD simulations

Table 1. Details of Each System for Hydrophobic Poly-I and Poly-II Polymers in Conjunction with 330 Charged Crowders[a]

	Poly-I				Poly-II			
system	N_w	N_c	$\langle l\rangle$	ρ	N_w	N_i	$\langle l\rangle$	ρ
water	30 000		9.954	0.997	30 000		9.662	0.994
CR+	31 370	330	9.958	1.000	31 330	330	9.970	1.000
CR−	31 370	330	9.922	1.007	31 330	330	9.913	1.007

[a] ϕ, N_w, and N_c represent the packing fraction in %, number of water molecules, and crowders involved in the system, respectively. $\langle l\rangle$ and ρ represent the average side length of the box in nanometer and average density of the system in g cm^{-3} obtained from the simulations.

https://doi.org/10.1021/acspolymersau.4c00011
ACS Polym. Au 2024, 4, 289−301

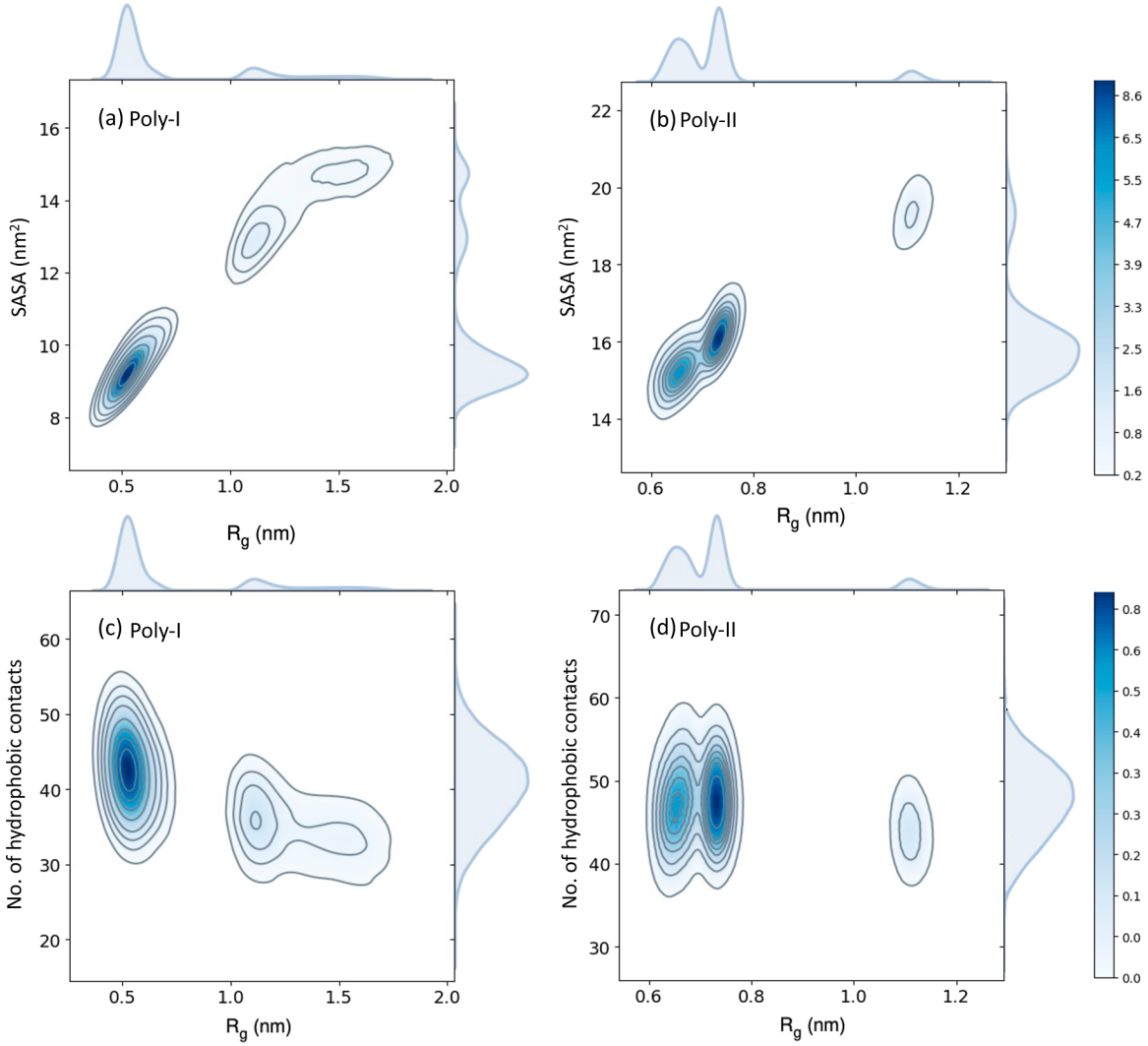

Figure 2. 2-D probability distributions (a,b) of SASA and radius of gyration (R_g) for Poly-I and Poly-II, respectively, and (c,d) of the number of hydrophobic contacts and R_g for Poly-I and Poly-II, respectively, in neat water.

were performed using the PLUMED 2.6.0 plugin. A harmonic wall potential was applied on R_g of the polymer with a cutoff of $R_g^{\#}$ = 1.075 nm for Poly-I and $R_g^{\#}$ = 0.8 nm for Poly-II. This potential acts on the polymer and biases the conformation to C-state if R_g > 1.075 nm (or 0.8 nm) and vice versa for the E-state. This ensured sufficient sampling of the C- and E-states of the polymers in the relevant ensemble. The equilibration and production runs were performed in an *NPT* ensemble with the parameters as described before. The production run was performed for 100 ns each for the C and E ensembles for each polymer. For analyzing the energetics, only those polymer conformations from the trajectory were considered which had zero bias wall potential.

For computing the preferential binding coefficient of the crowders (or the counterions), the following equation was used

$$\Gamma_{pc} = \langle n_c(r) - \frac{N_c - n_c(r)}{N_w - n_w(r)} n_w(r) \rangle \tag{8}$$

where N_x is the total number of water molecules or crowders (or counterions) in the system and $n_x(r)$ denotes the number of waters or crowders (or counterions) at a proximal distance, r, from the polymer surface. The proximal distance is the minimum distance between the center of mass of the crowder and the polymer surface.

The local tetrahedral order metric, q_{tet}, of water molecules is a measure of the tetrahedral network formed by the oxygen atoms of the water molecules. q_{tet} for oxygen atom i can be calculated as[50,51]

$$q_{tet} = 1 - \frac{3}{8} \sum_{j=1}^{3} \sum_{k=j+1}^{4} \left(\cos \psi_{jk} + \frac{1}{3} \right)^2 \tag{9}$$

where ψ_{jk} is the angle formed between bond vectors r_{ij} and r_{ik}, where the central oxygen atom, i, is surrounded by four nearest oxygen atoms labeled by j and k. If the tetrahedral network of water is perfectly ordered, q_{tet} = 1. The hydrophobic contact is defined between any two monomer beads of the polymer that are separated by 3 beads or more within a distance of 0.4 nm. The solvent-accessible surface area (SASA) is computed using GROMACS tool *gmx sasa*.

RESULTS

Polymer Collapse Equilibria in Water

First, we examine the conformational properties of the polymers in terms of the probability distributions of SASA and the number of hydrophobic contacts as a function of the radius of gyration (R_g) of the polymers, as shown in Figure 2. The two-dimensional (2-D) distributions show that both Poly-I and Poly-II exhibit the C-state and E-state of the polymer. As shown in Figure 2a,b, for Poly-I, the minima for the C-state appears around R_g = 0.55 nm and for the E-state appears around R_g = 1.5 nm with the increasing SASA values. For Poly-II, the C-state appears between R_g of 0.6 and 0.8 nm and the E-state appears around

https://doi.org/10.1021/acspolymersau.4c00011
ACS Polym. Au 2024, 4, 289−301

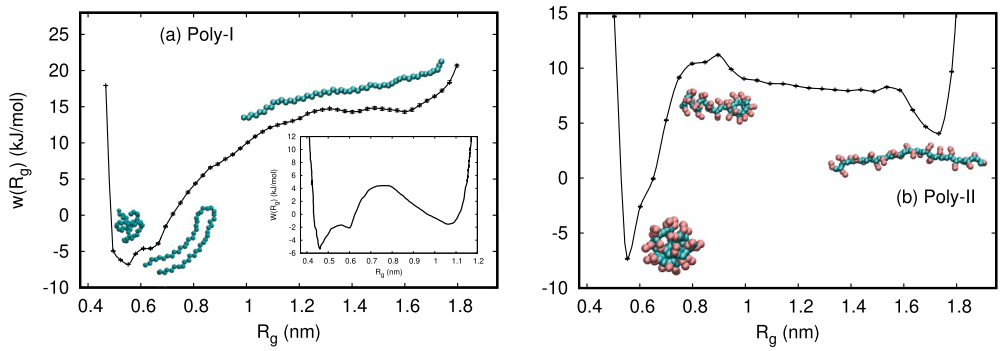

Figure 3. Potential of mean force profiles ($w(R_g)$) for (a) Poly-I and (b) Poly-II in pure water solution. The inset in (a) shows the profile for 32-mer linear polymer. The data for 32-mer polymer has been taken from ref 33. The snapshots are representative polymer conformations at different R_g values. The data for the inset figure has been taken with permission from ref 33. Copyright 2018 American Chemical Society.

R_g = 1.2 nm. Similarly, in Figure 2c,d, the number of hydrophobic contacts are higher for the C-state for both Poly-I and Poly-II, which decrease for the E-state. The two dense minima for the C- and E-states are separated by the free energy barrier that lies between R_g of 0.7 and 1.1 nm for Poly-I, whereas it lies between R_g of 0.8 and 1.1 nm for Poly-II. It is to be noted that the E-state of Poly-I is sampled until R_g = 1.8 nm, whereas for a similar chain length in Poly-II, it is sampled until R_g = 1.2 nm. This highlights the limitation of the MD simulation that is not able to sample fully stretched conformations of Poly-II. To circumvent this insufficient conformational sampling, we adhere to the umbrella sampling simulations to generate the pmf profiles of these polymers.

The pmf profiles for the two polymers in pure aqueous solutions (without crowders) are shown in Figure 3. Both polymers show qualitatively distinct pmf profiles. As shown in Figure 3a, the linear polymer, Poly-I, strongly favors the C-state over the E-state as is indicated by the deep minimum for the C-state around R_g = 0.55 nm corresponding to the compact globule conformation of the polymer. An additional shoulder minimum is observed around R_g = 0.65 nm, which corresponds to the hairpin-shaped conformation of the polymer. The E-state minimum is observed around R_g = 1.6 nm which is not well defined, indicating that the E-state is marginally stable. Such a pmf profile for hydrophobic polymers with marginally stable E-state has also been found in previous studies.[52,53] The inset of Figure 3a shows the pmf profile of the 32-mer linear polymer examined in our previous study.[33] Increasing the chain length results in a qualitatively different pmf profile. The primary differences lie in the E-state being less favorable in 50-mer Poly-I than in the 32-mer polymer and the barrier becoming less distinct in the Poly-I solution. In the case of the second polymer solution, Poly-II, the pmf profile shows a deep minimum for the C-state and a well-separated minimum for the E-state, as shown in Figure 3b. The minimum for the C-state occurs at R_g = 0.55 nm. The E-state minimum is observed at R_g = 1.7 nm, higher than that observed for the E-state of Poly-I. There is a well-defined barrier in the profile of Poly-II that distinctly separates the C- and E-states unlike that observed for Poly-I. From Figures 2 and 3, it can be seen that for Poly-I, a suitable choice of cutoff R_g would be 1 nm and that for Poly-II would be 0.8 nm. The differences in the widths of the C-state minimum in the pmf profiles of the two polymers indicate that Poly-I has more conformational flexibility in the C-state (broader minimum) than Poly-II (narrower minimum). This indicates that Poly-II has a lower conformational entropy as compared to Poly-I.

The free energies of polymer collapse ($\Delta G^{E\to C}$) for both Poly-I and Poly-II are computed from the pmf profiles and are found to be −15.59 and −7.50 kJ mol^{-1}, respectively, in neat water. This indicates that it is highly favorable for Poly-I to collapse in water as compared to that for Poly-II. Interestingly, the 32-mer linear hydrophobic polymer was found to be sparingly soluble in water with $\Delta G^{E\to C}$ = −2.0 kJ mol^{-1} in our previous study.[33] This underscores an intriguing observation that on modifying the architecture of the polymer in terms of increasing the number of monomers or including side chains to the polymer, it significantly affects $\Delta G^{E\to C}$. The hydrophobic collapse of the polymer is observed to be enhanced in Poly-I more than in Poly-II even when there are more hydrophobic beads in Poly-II. Introducing the side chains in Poly-II induces steric effects, favoring the E-state formation (more than in Poly-I) which leads to an increase in $\Delta G^{E\to C}$.

In order to understand this further, we examine the change in polymer−solvent energy ($\Delta E_{pv}^{E\to C}$) and entropy change ($\Delta S_{pv}^{E\to C}$) on polymer collapse. For Poly-I, $\Delta E_{pv}^{E\to C}$ is found to be 3.55 kJ mol^{-1} and $-T\Delta S_{pv}^{E\to C}$ is found to be −19.99 kJ mol^{-1}. This indicates that the polymer collapse in water is opposed by $\Delta E_{pv}^{E\to C} > 0$ but is favored by $-T\Delta S_{pv}^{E\to C} < 0$(or $\Delta S_{pv}^{E\to C} > 0$). This is due to the gain in degrees of freedom of water molecules that are released from the polymer solvation shell on the collapse of the polymer. The polymer collapse is associated with an energetic penalty as losing contacts with water molecules on collapse leads to an increase in $\Delta E_{pv}^{E\to C}$. The thermodynamic driving forces for collapse of Poly-I are similar to those underlying 32-mer polymer collapse in water as discussed in our previous study.[33] $\Delta S_{pv}^{E\to C}$ is found to be similar for the two polymers; however, $\Delta E_{pv}^{E\to C}$ is much higher for the 32-mer polymer (23 kJ mol^{-1}). The sharp decrease in $\Delta G^{E\to C}$, therefore, arises due to the lower energetic penalty for Poly-I collapse. This may be due to the fact that the intrapolymer energy change ($\Delta E_{pp}^{E\to C}$) on polymer collapse is more favorable for Poly-I as compared to the 32-mer polymer. This reduces the energetic penalty for polymer collapse for Poly-I and results in a highly favorable $\Delta G^{E\to C}$. On the other hand, the collapse of Poly-II is opposed by $-T\Delta S_{pv}^{E\to C} > 0$ (i.e., ≈40 kJ mol^{-1} or $\Delta S_{pv}^{E\to C} < 0$) but is favored by $\Delta E_{pv}^{E\to C} < 0$ (−50 kJ mol^{-1}) that drives the collapse. Examining the components of $\Delta E_{pv}^{E\to C}$ shows that the polymer−water energy change ($\Delta E_{pw}^{E\to C} > 0$) is unfavorable for

https://doi.org/10.1021/acspolymersau.4c00011
ACS Polym. Au 2024, 4, 289−301

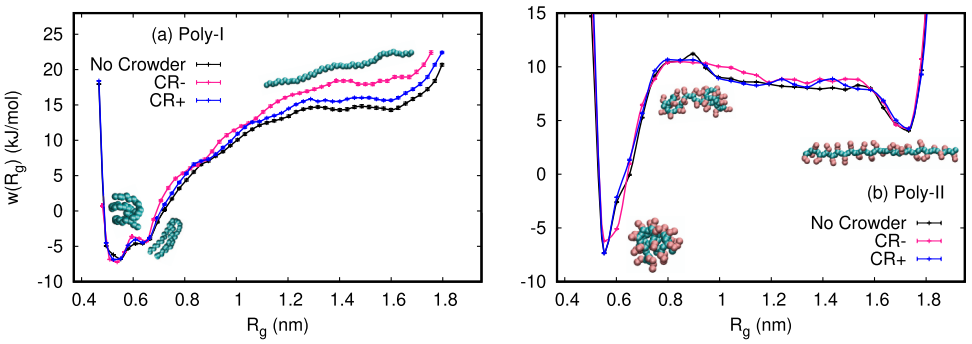

Figure 4. Potential of mean force profiles ($w(R_g)$) for (a) Poly-I and (b) Poly-II in aqueous solutions of anionic and cationic crowders. The snapshots are representative polymer conformations at different R_g values.

both Poly-I and Poly-II (slightly more for Poly-I) due to the loss of water contacts on collapse of the polymer (see Figure 9b). However, the second contribution to $\Delta E_{pv}^{E\to C}$ comes from the intrapolymer energy change ($\Delta E_{pp}^{E\to C} < 0$) which is more favorable for Poly-II than for Poly-I. This is due to the additional side chains in Poly-II that lead to favorable intrapolymer interactions that drive the collapse. This contribution makes the overall $\Delta E_{pv}^{E\to C} < 0$ for Poly-II and therefore is the primary driving force for polymer collapse in water.

Polymer Collapse in Charged Crowded Solutions

Figure 4 shows the pmf profiles of the linear and branched polymers in the presence of the charged crowders, i.e., positively charged (CR+) and negatively charged (CR−) crowders. Poly-I shows qualitatively similar pmf profiles in CR+ and CR− crowder solutions (Figure 4a). The minimum at R_g = 0.55 nm for the collapsed state is highly preferred with a small shoulder at R_g = 0.65 nm even in the crowded solutions. Interestingly, the preference for the E-state varies in all the crowded solutions when compared with no crowder solution. The preference for the E-state in different crowded solutions follows the order CR− < CR+< pure-water solutions. Such differences in the preference for the E-state lead to different $\Delta G^{E\to C}$ values as shown in Figure 5. The $\Delta G^{E\to C}$ follows the order (most favorable to least favorable for collapse) CR−, CR+, pure-water. Figure 4b shows the pmf profiles of Poly-II where two distinct minima are observed in all the crowded solutions, similar to that observed in the pure water solution. The C-state is observed at R_g = 0.55 nm, with a shoulder minimum around R_g = 0.65 nm. The E-state is observed around R_g = 1.7 nm, similar to that observed in the pure water solution. Due to similar preferences for the C- and E-states in crowded solutions, $\Delta G^{E\to C}$ is found to be not significantly different in the crowded solutions, as shown in Figure 5.

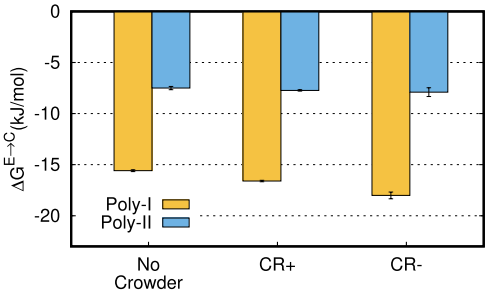

Figure 5. Collapse free energy ($\Delta G^{E\to C}$) of Poly-I and Poly-II in aqueous solutions of anionic and cationic crowders.

In order to understand these differences further, we examine the preferential binding coefficients of the crowders on the polymer surface, as shown in Figure 6. The crowder molecules are found to preferentially adsorb on both Poly-I and Poly-II since $\Gamma > 0$ in both C- and E-states. For both the polymers, $\Gamma(C) > \Gamma(E)$ indicates that the polymer collapse equilibrium would shift to the C-state in these crowded solutions. However, there is a preferential depletion of the crowders ($\Gamma < 0$) very close to the polymer surfaces at a proximal distance of ≈0.35 nm for both the polymers, beyond which the crowders preferentially adsorb on the polymer surface. This implies that a thin hydration layer is formed on the polymer surface in the crowded solutions, which is further solvated by the adsorption of the crowders. The counterions are weakly bound to the polymer surface as can be seen in Figure 6c−h. To further understand the molecular mechanisms for polymer collapse, we investigate the contributions of change in polymer−solvent energy ($\Delta E_{pv}^{E\to C}$) and entropy ($\Delta S_{pv}^{E\to C}$) to the collapse free energy. For Poly-I, Figure 7a shows that $-T\Delta S_{pv}^{E\to C} < 0$(or $\Delta S_{pv}^{E\to C} > 0$) that favors polymer collapse in CR+ and CR− solutions. $\Delta S_{pv}^{E\to C}$ is more favorable for the crowded solutions relative to that in pure water. However, $\Delta E_{pv}^{E\to C} > 0$ implies that the polymer−solvent energy change opposes polymer collapse in crowded solutions. The energetic penalty, however, is higher in CR+ solution relative to that in pure water and CR− solutions. The energetic penalty primarily arises due to the loss of water contacts with the polymer on collapse as indicated by the unfavorable $\Delta E_{pw}^{E\to C} > 0$ (Figure 7b). The dehydration energy penalty decreases on going from CR+ to CR− solution. On polymer collapse, the loss in crowder molecules from the polymer solvation shell to the bulk is not significant as indicated by almost no change in polymer−crowder energy ($\Delta E_{pc}^{E\to C} \approx 0$). The intrapolymer energy change ($\Delta E_{pp}^{E\to C} < 0$) is, however, favorable for polymer collapse but not sufficient to overcome the dehydration energy penalty that makes the overall $\Delta E_{pv}^{E\to C} > 0$ unfavorable for collapse of Poly-I. This energetic penalty is overcome by the favorable $\Delta S_{pv}^{E\to C} > 0$ that arises due to the gain in entropic degrees of freedom of water molecules that are released into the bulk on polymer collapse. $\Delta S_{pv}^{E\to C} > 0$. This entropy gain is related to the fluctuations in the polymer−solvent interaction energy as described in the Methods section. The negatively charged

https://doi.org/10.1021/acspolymersau.4c00011
ACS Polym. Au 2024, 4, 289−301

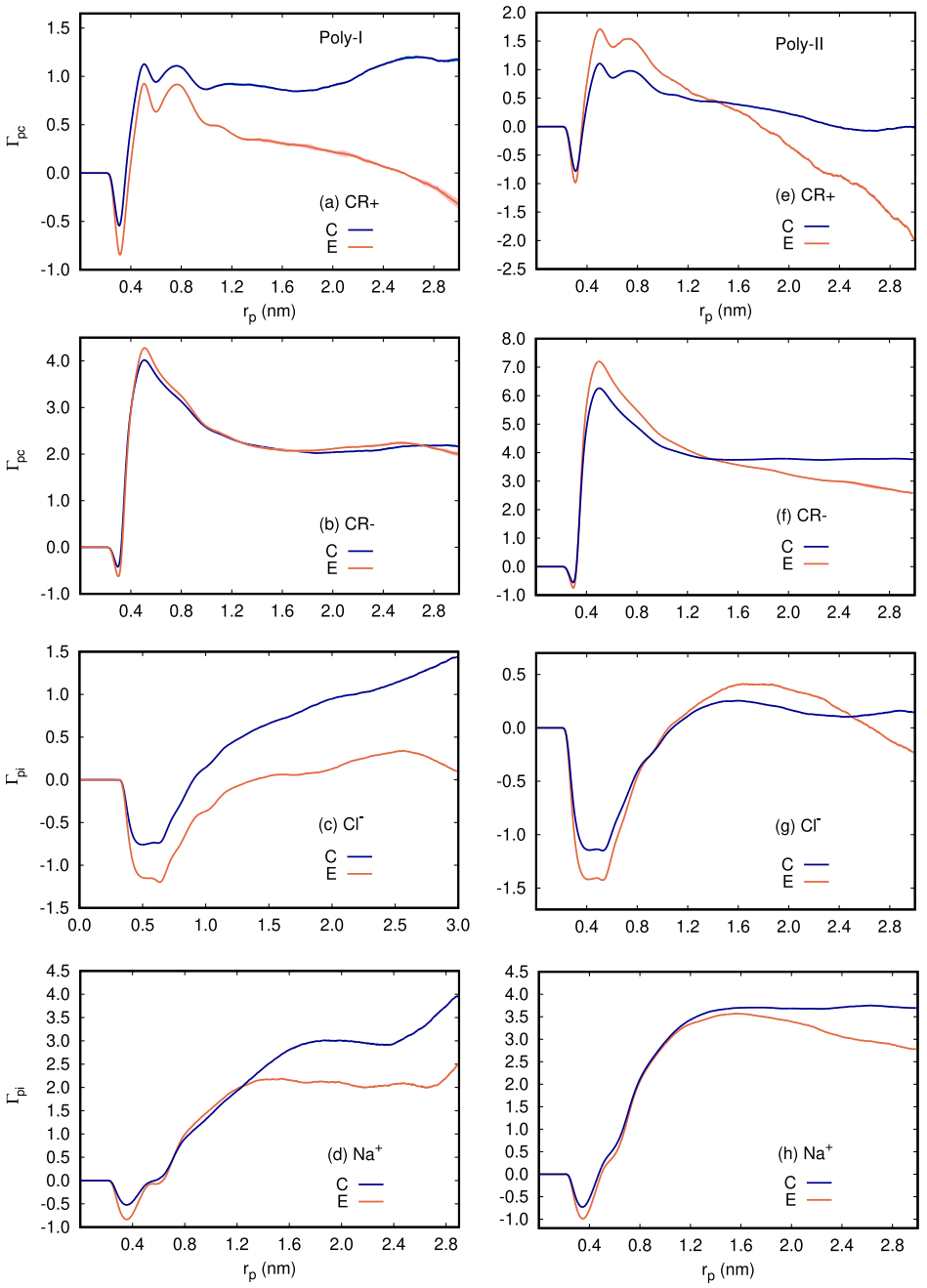

Figure 6. Preferential binding coefficients of (a,e) CR+, (b,f) CR−, (c,g) Cl^-, and (d,h) Na^+ as a function of proximal distance *r* from the surface of Poly-I and Poly-II, respectively.

beads of the CR− attract and orient the water dipoles toward the crowders, leading to a large accumulation of water molecules and anionic crowders near the polymer surface in both C- and E-states (see Figure 8a,c). The CR− crowders interact favorably via uncharged beads with the polymer surface in both E- and C-states. Therefore, CR− act like surfactant molecules that have favorable interactions with water, and they can screen the nonpolar polymer interface from water which decreases the dehydration energy penalty (decrease in $\Delta E_{pw}^{E\to C}$). The polymer collapse is also not accompanied by a high loss of polymer−crowder contacts as indicated by $\Delta E_{pc}^{E\to C} \approx 0$. Also, there is an increase in the intrapolymer energy change ($\Delta E_{pp}^{E\to C}$) on collapse relative to that in neat water. This could be due to the existence of partially extended E-state instead of fully extended E-state which is highly unstable (relative to neat water solution) and tends to collapse (as also indicated by the E-state minimum in the pmf profile, which is less stable in Figure 4a). This makes the overall $\Delta E_{pc}^{E\to C}$ unfavorable for collapse. It is also observed that the CR− accumulate at the central region of the polymer, preferably where the tetrahedral order of water molecules is lower than that of waters around the termini of the polymer, as shown in Figure 8d. In case of CR+, the crowders can interact favorably with the polymer surface via uncharged beads. Since the water dipoles point away from the cationic crowders, these crowders are very weakly hydrated, as shown in Figure 8b,c. On polymer collapse, this results in higher dehydration energy penalty than in CR− solution, i.e., the loss

https://doi.org/10.1021/acspolymersau.4c00011
ACS Polym. Au 2024, 4, 289−301

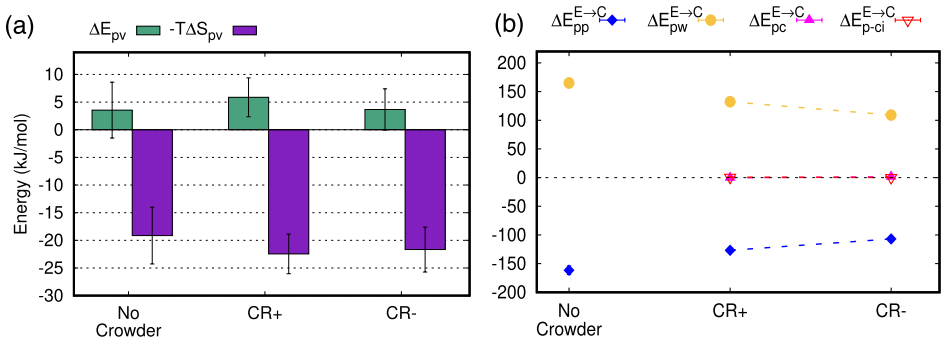

Figure 7. (a) Change in polymer−solvent energy ($\Delta E_{pv}^{E\to C}$) and entropy ($\Delta S_{pv}^{E\to C}$) on collapse of Poly-I in crowded aqueous solutions. (b) Change in intrapolymer ($\Delta E_{pp}^{E\to C}$), polymer−water ($\Delta E_{pw}^{E\to C}$), polymer−crowder ($\Delta E_{pc}^{E\to C}$), and polymer−counterion ($\Delta E_{p-ci}^{E\to C}$) energy to the total polymer−solvent energy change on polymer collapse.

in polymer−water contacts is higher than in case of CR− solution. Similar to CR−, the CR+ molecules preferentially bind to the central region of the polymer, where the water structuring is disordered as compared to the termini of the polymer (see Figure 8e). However, the number of crowders adsorbing on the polymer surface are much lesser than CR+. Therefore, the hydrophobic collapse is observed to be strengthened in the CR− solution to a higher extent than in CR+ solution.

In the case of Poly-II, the collapse free energy is found to be not significantly different in the crowded solutions. It is slightly more favorable for the polymer to collapse in CR− solution than in CR+ solution. Similar to that observed in pure water solution, polymer collapse is opposed by $-T\Delta S_{pv}^{E\to C} > 0$ (or $\Delta S_{pv}^{E\to C} < 0$) in both CR+ and CR− solutions, with higher entropic penalty in the case of CR+ solution (Figure 9). This is, however, overcompensated by the favorable $\Delta E_{pv}^{E\to C} < 0$ in both the crowder solutions. The unfavorable polymer−water energy change ($\Delta E_{pw}^{E\to C} > 0$) and unfavorable polymer−crowder energy change ($\Delta E_{pc}^{E\to C} > 0$) oppose the collapse. Reduction of polymer−water and polymer−crowder contacts on polymer collapse is unfavorable. This is because the crowders preferentially adsorb and interact favorably via van der Waals interactions with both C- and E-states of the polymer, with higher contacts with the E-state. On polymer collapse, a loss in polymer−water and polymer−crowder contacts leads to a higher energetic penalty that opposes collapse. However, the intrapolymer energy change ($\Delta E_{pp}^{E\to C} < 0$) is highly favorable for polymer collapse in both the crowder solutions which makes the overall $\Delta E_{pv}^{E\to C} < 0$ and favorable for polymer collapse in both the crowder solutions. Such favorable intrapolymer energy on polymer collapse also results in lower conformational entropy of the polymer and therefore $\Delta S_{pv}^{E\to C} < 0$. However, among the two crowders, $\Delta E_{pp}^{E\to C}$ is more favorable in CR+ solution. CR− seem to interact more favorably (than CR+) with the E-state of Poly-II than with the C-state due to which $\Delta E_{pc}^{E\to C}$ on polymer collapse is more unfavorable for CR− than for CR+. Also, the hydration energy penalty ($\Delta E_{pw}^{E\to C}$) is lesser in the case of CR− solution than in CR+ solution, similar to that observed for Poly-I. This implies that there is lesser loss in the number of polymer−water contacts and larger loss in the number of polymer−crowder contacts on collapse in Poly-II (as also indicated in Figure 10a,c). This results in the entropic penalty of collapse being smaller in the case of CR− solution. This leads to slightly more favorable collapse free energy of the polymer in CR− solution when compared with CR+ or in pure water. It is interesting to note the role of the polymer−crowder energy in the case of Poly-II. The loss of crowder molecules on polymer collapse is unfavorable that is reflected in the increasing and positive $\Delta E_{pc}^{E\to C}$. Such an unfavorable change in $\Delta E_{pc}^{E\to C}$ was not observed in Poly-I, where there were equal number of crowders in C- and E-states. It seems that the loss of crowders is easier from the solvation shell of Poly-II. This can be understood in terms of the crowder interaction with the side chain versus backbone of Poly-II as shown in Figure 10c. The CR− are found to be interacting weakly with higher probability with the side chains such that they are loosely bound to the side chains in both the C- and E-states. This was not the case for Poly-I. Therefore, the loss in the number of crowders on Poly-II collapse is higher and leads to an increase in $\Delta E_{pc}^{E\to C}$. The CR+ molecules also interact more favorably with the side chains than the backbone in the C- and E-states, however, with lesser probability than the CR− molecules as can be seen in Figure 10b,c. Moreover, both crowders induce equal disordering of water molecules around the termini or around the side chains of the central region of Poly-II (see Figure 10d,e).

DISCUSSION AND CONCLUSIONS

In this study, we have compared the effects of the charged hydrophobic cosolutes at crowded concentrations on the hydrophobic collapse of two polymers: one that is linear and the other that has side chains. The results provide the following interesting insights: (1) Poly-I favors collapse more than in Poly-II in neat water, as indicated by the collapse free energies, even though there are more hydrophobic groups (side chains) on Poly-II. (2) The anionic crowders discriminate between the two polymers in terms of strengthening the hydrophobic collapse. Addition of anionic CR− crowders to an aqueous solution of Poly-I strengthens the hydrophobic collapse to a higher extent. However, for the case of Poly-II which has more hydrophobic groups, it can be seen that the polymer collapse free energy is only slightly favored in any crowder solution when compared to that in pure water solution. (3) The thermodynamic driving forces underlying the polymer collapse are distinct for the two polymers. Poly-I collapse is supported by the polymer−solvent entropy change, whereas the collapse of Poly-II is supported by the polymer−solvent energy change. The side chains provide a

https://doi.org/10.1021/acspolymersau.4c00011
ACS Polym. Au 2024, 4, 289−301

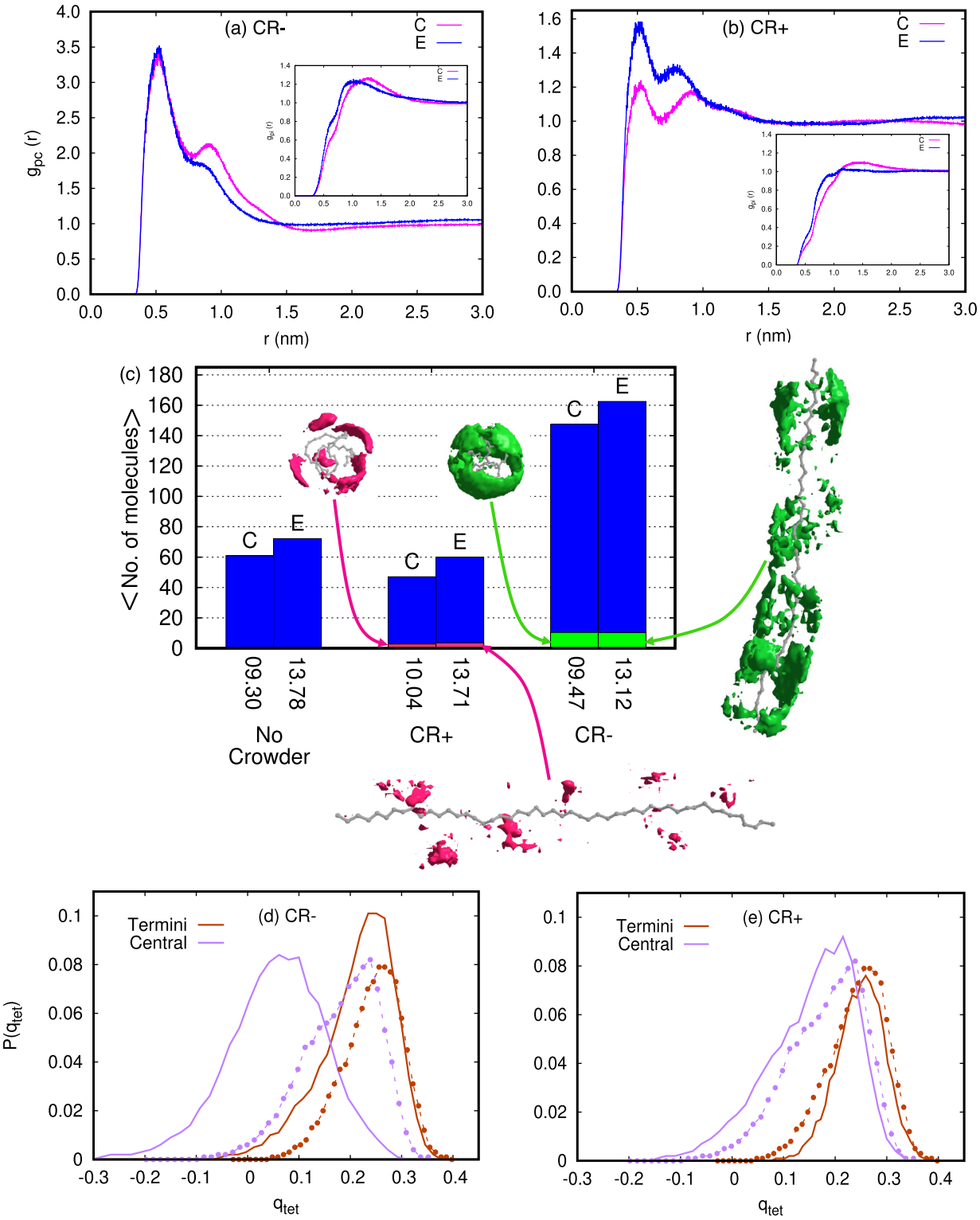

Figure 8. (a) Radial distribution function of the polymer−crowder interaction for (a) CR− and (b) CR+ in the C- and E-states of Poly-I. (c) Average number of water molecules and crowder molecules in the first solvation shell of Poly-I. The numbers of the *x*-axis denote the average SASA (nm^2) of Poly-I in different aqueous solutions. The snapshots show the spatial density function of the crowders in first solvation shell of C- and E-states of Poly-I. (d,e) Probability distributions of tetrahedral order ($P(q_{tet})$) of water molecules around the termini and the central region of Poly-I in the E-state in the first solvation shell in CR− and CR+ solutions, respectively. The solid lines and dotted lines represent solutions with crowders and no crowders, respectively.

higher accessible surface to the solvent in Poly-II that results in different thermodynamic forces. (4) This indicates that the charged crowded environment need not necessarily enhance the hydrophobic collapse; it is rather determined by the weak or strong hydration of the crowders that in turn affect the hydration of the polymer. Weakly hydrated cationic crowders do not stabilize the C-state more favorably than the strongly hydrated anionic crowders. Anionic crowders strengthen the hydrophobic

https://doi.org/10.1021/acspolymersau.4c00011
ACS Polym. Au 2024, 4, 289−301

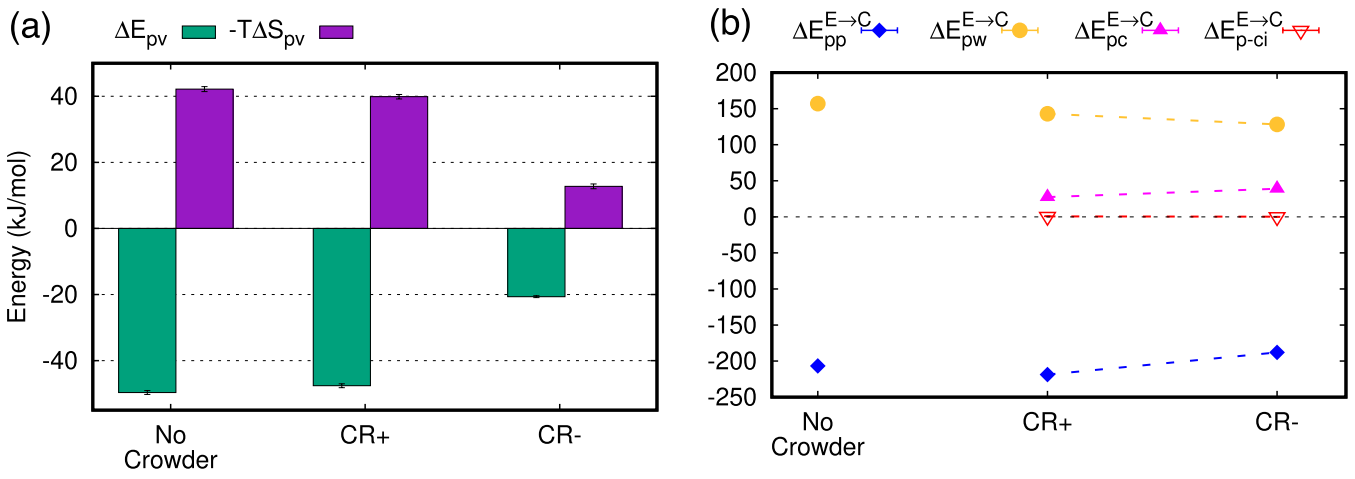

Figure 9. (a) Change in polymer−solvent energy ($\Delta E_{pv}^{E\rightarrow C}$) and entropy ($\Delta S_{pv}^{E\rightarrow C}$) on collapse of Poly-II in crowded aqueous solutions. (b) Change in intrapolymer ($\Delta E_{pp}^{E\rightarrow C}$), polymer−water ($\Delta E_{pw}^{E\rightarrow C}$), polymer−crowder ($\Delta E_{pc}^{E\rightarrow C}$), and polymer−counterion ($\Delta E_{p-ci}^{E\rightarrow C}$) energy to the total polymer−solvent energy change on polymer collapse.

collapse when they interact with the polymer backbone (Poly-I). Like surfactants, the anionic crowders screen the nonpolar polymer surface while interacting favorably with the water molecules that get released on polymer collapse. This strengthens the hydrophobic collapse in the polymer via the entropic mechanism. When the side chains are introduced in Poly-II, the anionic crowders loosely bind to the side chains more preferably than to the backbone, resulting in a loss of crowders as well as waters on collapse. This decreases the entropic penalty, which is still high to oppose the collapse. The favorable intrapolymer energy on collapse makes the overall polymer−solvent energy favorable for collapse, although this does not lead to a significant strengthening of the hydrophobic collapse in Poly-II. (5) The propensity of anionic crowders to preferentially adsorb on the side chains or the backbone is found to be determined by the structuring of water molecules around the different regions of the polymer. (6) The well-known aggregating effect of crowding is found to be dependent on the architecture of the polymers. It is strengthened in the case of the linear polymer and weakened in the case of the branched polymer.

Our observations are consistent with the results shown by Chudoba et al.[40] where they found that the weakly interacting anion decreases the LCST of the uncharged polymer or in other words, enhances the salting-out of the polymer. In another study, Heyda et al. showed that GndSCN had the highest propensity to salt-out the ELP (Elastin-like peptide) at low concentrations when compared with $GndSO_4$[43] and to salt-out the PNIPAM (poly-N-isopropyl acrylamide) polymer.[41] The SCN^- was found to preferentially bind on ELP (or PNIPAM surface), whereas SO_4^{2-} was found to be weakly bound to ELP and depleted from the PNIPAM surface. Although, SCN^- destabilized the peptide, the counterion Gnd^+ was found to stabilize it. Strongly hydrated cations such as Ca^{2+}, Mg^{2+}, and Li^+ have been found to be weakly binding with the peptides.[41] This is a similar observation as we have found in our work where CR− is more effective than CR+ to induce polymer collapse. They also pointed out that in order to understand the salting-in and salting-out effects, one needs to examine the interactions of the cations and anions not only with water but also with the biomolecular surfaces.[41] They showed that the weakly hydrated anions and strongly hydrated cations are attracted toward the protein backbone and are effective in salting-out the protein. This is contrary to what is observed in our study, where the weakly hydrated anionic crowder interacts more favorably with the hydrophobic side chains of the polymer rather than the hydrophobic backbone and strengthens the polymer collapse. Okur et al. also indicated that the weakly hydrated anions such as SCN− partition to the hydrophobic interface more easily since they can shed their hydration shell to preferentially adsorb on the surface.[41] Previous studies have also shown that weakly hydrated I^- tend to interact more favorably with the nonpolar alanine residues and induced destabilization of the peptide by amplifying the action of the cations.[54] In another study, polymerization or cooperative self-assembly of a bacterial protein, FtsZ, was seen to be accelerated in the presence of negatively charged DNA at crowded concentration.[55]

The water structure around the termini and the side chains of the polymers is also found to play a key role in determining the discriminating behavior of the anionic crowders. Rogers et al. showed that the weakly hydrated ions such as SCN^- have a tendency to preferentially bind to the central region of poly(ethylene oxide) where the structuring of water was disordered as compared to the polymer termini where the water was more ordered.[44] Our results also show that in the case of the linear Poly-I, the anionic crowders preferentially adsorb in the central region of the polymer where the tetrahedral order of waters is slightly lower than that found around the termini of the polymer. In the case of Poly-II, the water molecules are equally disordered around the side chains in the central region or around the termini of the polymer, thereby leading to loss of binding of the crowders around the polymer. The results underscore the sensitivity of the weakly charged crowded environment in strengthening or weakening the hydrophobic collapse in polymers based on their architecture. Such insights have implications for designing crowding-sensitive smart materials for tailored biomedical applications. To summarize, the insights provide a fundamental understanding of the thermodynamic driving forces underlying the crowding effects of charged cosolutes on the hydrophobic collapse of the two polymers. The results highlight an emerging view of molecular crowding, where the aggregating effect of crowding is found to be sensitive to the polymer architecture. The findings have implications for strategizing the employability of the crowded environment as

https://doi.org/10.1021/acspolymersau.4c00011
ACS Polym. Au 2024, 4, 289−301

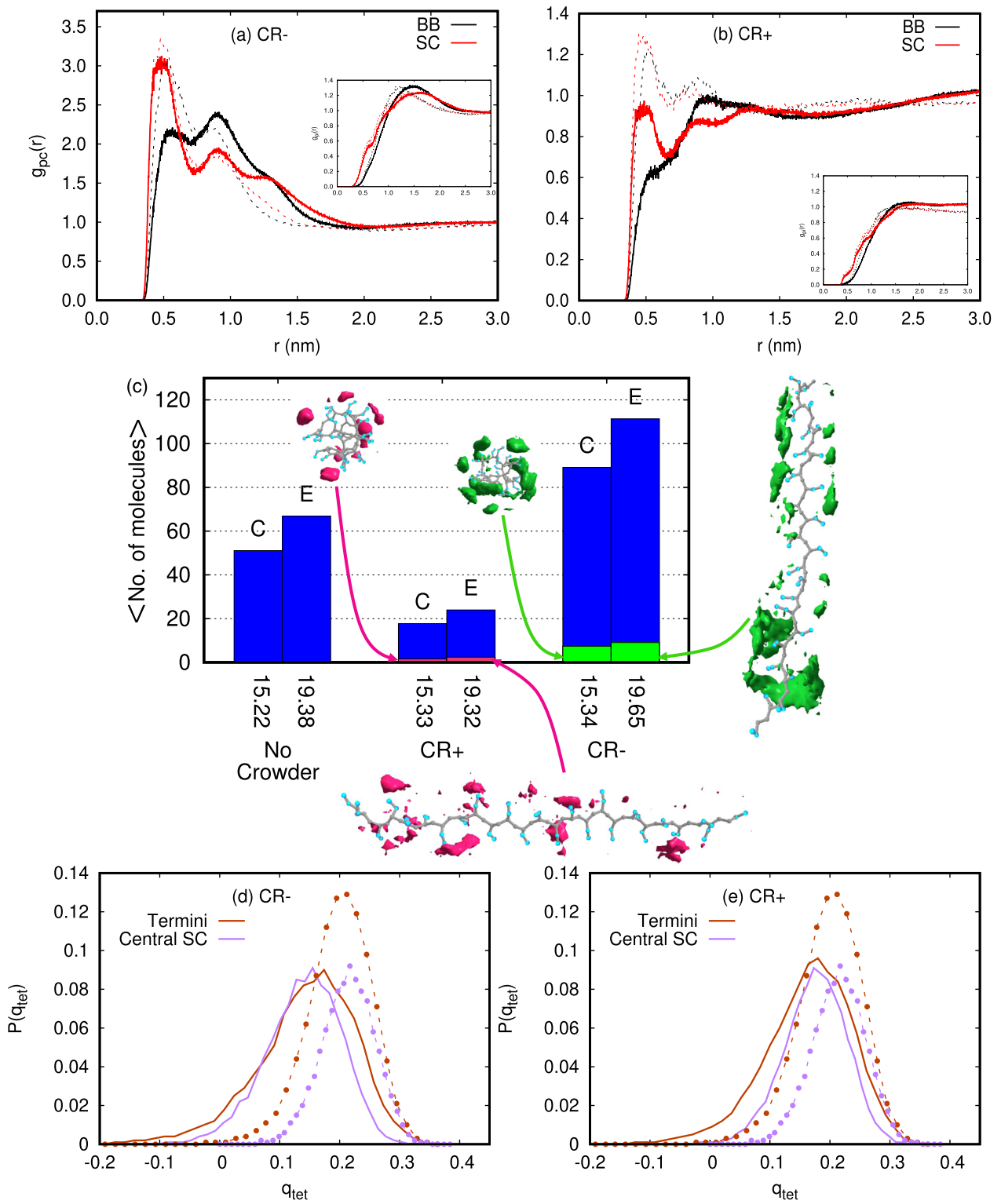

Figure 10. (a) Radial distribution function of polymer−crowder interaction for (a) CR− and (b) CR+ in the C- and E-states of Poly-II. (c) Average number of water molecules and crowder molecules in the first solvation shell of Poly-II. The numbers of the *x*-axis denote the average SASA (nm^2) of Poly-II in different aqueous solutions. The snapshots show the spatial density function of the crowders in the first solvation shell of the C- and E-states of Poly-II. (d,e) Probability distributions of tetrahedral order ($P(q_{tet})$) of water molecules around the termini and the side chains of the central region of Poly-II in the E-state in the first solvation shell in CR− and CR+ solutions, respectively. The solid lines and dotted lines represent solutions with crowders and no crowders, respectively.

a tool in designing tunable responsive polymer-based smart materials for biomedical applications.

https://doi.org/10.1021/acspolymersau.4c00011
ACS Polym. Au 2024, 4, 289−301

AUTHOR INFORMATION

Corresponding Author

Divya Nayar − *Department of Materials Science and Engineering, Indian Institute of Technology Delhi, New Delhi 110016, India;* orcid.org/0000-0001-8569-7633; Email: divyanayar@mse.iitd.ac.in

Author

Satyendra Rajput − *Department of Materials Science and Engineering, Indian Institute of Technology Delhi, New Delhi 110016, India*

Complete contact information is available at: https://pubs.acs.org/10.1021/acspolymersau.4c00011

Author Contributions

CRediT: **Satyendra Rajput** data curation, formal analysis, investigation, methodology, writing-review & editing; **Divya Nayar** conceptualization, funding acquisition, project administration, resources, supervision, writing-original draft.

Notes

The authors declare no competing financial interest.

ACKNOWLEDGMENTS

S.R. thanks the Indian Institute of Technology Delhi for the Senior Research Fellowship. D.N. acknowledges the financial support from SERB for a Startup Research Grant (SRG/2021/000804). The authors acknowledge IIT Delhi HPC facility for the computational resources.

REFERENCES

(1) Ben-Naim, A. *Hydrophobic Interactions*; Plenum: New York, 1980.
(2) Dill, K. A. Dominant Forces in Protein Folding. *Biochemistry* **1990**, *29*, 7133−7155.
(3) Hummer, G.; Garde, S.; García, A.; Pratt, L. R. New Perspectives on Hydrophobic Effects. *Chem. Phys.* **2000**, *258*, 349−370.
(4) Pratt, L. R. Molecular Theory of Hydrophobic Effects: "She is too Mean to Have her Name Repeated. *Annu. Rev. Phys. Chem.* **2002**, *53*, 409−436.
(5) Chandler, D. Interfaces and the driving force of hydrophobic assembly. *Nature* **2005**, *437*, 640−647.
(6) Chiti, F.; Dobson, C. M. Protein Misfolding, Functional Amyloid, and Human Disease. *Annu. Rev. Biochem.* **2006**, *75*, 333−366.
(7) Ben-Amotz, D. Water-Mediated Hydrophobic Interactions. *Annu. Rev. Phys. Chem.* **2016**, *67*, 617−638.
(8) Stuart, M. A. C.; Huck, W. T.; Genzer, J.; Müller, M.; Ober, C.; Stamm, M.; Sukhorukov, G. B.; Szleifer, I.; Tsukruk, V. V.; Urban, M.; et al. Emerging applications of stimuli-responsive polymer materials. *Nat. Mater.* **2010**, *9*, 101−113.
(9) Hoffman, A. S. The origins and evolution of "controlled" drug delivery systems. *J. Controlled Release* **2008**, *132*, 153−163.
(10) Mendes, P. M. Stimuli-responsive surfaces for bio-applications. *Chem. Soc. Rev.* **2008**, *37*, 2512−2529.
(11) Alexander, C.; Shakesheff, K. M. Responsive polymers at the biology/materials science interface. *Adv. Mater.* **2006**, *18*, 3321−3328.
(12) Ellis, R. J. Macromolecular crowding: An important but neglected aspect of the intracellular environment. *Curr. Opin. Struct. Biol.* **2001**, *11*, 114−119.
(13) Ellis, R.; Minton, A. P. Cell biology: join the crowd. *Nature* **2003**, *425*, 27−28.
(14) Zimmerman, S. B.; Minton, A. P. Macromolecular Crowding: Biochemical, Biophysical, and Physiological Consequences. *Annu. Rev. Biophys. Biomol. Struc.* **1993**, *22*, 27−65.
(15) Zhou, H.-X.; Rivas, G.; Minton, A. P. Macromolecular Crowding and Confinement: Biochemical, Biophysical, and Potential Physiological Consequences. *Annu. Rev. Biophys.* **2008**, *37*, 375−397.
(16) Zimmerman, S.; Trach, S. Estimation of macromolecule concentrations and excluded volume effects for the cytoplasm of Escherichia coli. *J. Mol. Biol.* **1991**, *222*, 599−620.
(17) Asakura, S.; Oosawa, F. Interaction between particles suspended in solutions of macromolecules. *J. Polym. Sci.* **1958**, *33*, 183−192.
(18) Bhat, R.; Timasheff, S. N. Steric exclusion is the principal source of the preferential hydration of proteins in the presence of polyethylene glycols. *Protein Sci.* **1992**, *1*, 1133−1143.
(19) Senske, M.; Törk, L.; Born, B.; Havenith, M.; Herrmann, C.; Ebbinghaus, S. Protein Stabilization by Macromolecular Crowding through Enthalpy Rather Than Entropy. *J. Am. Chem. Soc.* **2014**, *136*, 9036−9041.
(20) Benton, L. A.; Smith, A. E.; Young, G. B.; Pielak, G. J. Unexpected Effects of Macromolecular Crowding on Protein Stability. *Biochemistry* **2012**, *51*, 9773−9775.
(21) Feig, M.; Sugita, Y. Variable Interactions between Protein Crowders and Biomolecular Solutes Are Important in Understanding Cellular Crowding. *J. Phys. Chem. B* **2012**, *116*, 599−605.
(22) Mukherjee, S. K.; Gautam, S.; Biswas, S.; Kundu, J.; Chowdhury, P. K. Do Macromolecular Crowding Agents Exert Only an Excluded Volume Effect? A Protein Solvation Study. *J. Phys. Chem. B* **2015**, *119*, 14145−14156.
(23) Sapir, L.; Harries, D. Is the depletion force entropic? Molecular crowding beyond steric interactions. *Curr. Opin. Colloid Interface Sci.* **2015**, *20*, 3−10.
(24) Nayar, D. Small crowder interactions can drive hydrophobic polymer collapse as well as unfolding. *Phys. Chem. Chem. Phys.* **2020**, *22*, 18091−18101.
(25) Nayar, D. Molecular Crowders Can Induce Collapse in Hydrophilic Polymers via Soft Attractive Interactions. *J. Phys. Chem. B* **2023**, *127*, 6265−6276.
(26) Olgenblum, G. I.; Carmon, N.; Harries, D. Not Always Sticky: Specificity of Protein Stabilization by Sugars Is Conferred by Protein-Water Hydrogen Bonds. *J. Am. Chem. Soc.* **2023**, *145*, 23308−23320.
(27) Stewart, C. J.; Olgenblum, G. I.; Propst, A.; Harries, D.; Pielak, G. J. Resolving the Enthalpy of Protein Stabilization by Macromolecular Crowding. *Protein Sci.* **2023**, *32*, No. e4573.
(28) Ostrowska, N.; Feig, M.; Trylska, J. Varying molecular interactions explain aspects of crowder-dependent enzyme function of a viral protease. *PLoS Comput. Biol.* **2023**, *19*, No. e1011054.
(29) Garg, H.; Rajesh, R.; Vemparala, S. The conformational phase diagram of neutral polymers in the presence of attractive crowders. *J. Chem. Phys.* **2023**, *158*, 14903.
(30) Sarkar, M.; Lu, J.; Pielak, G. Protein Crowder Charge and Protein Stability. *Biochemistry* **2014**, *53*, 1601−1606.
(31) Canchi, D. R.; García, A. E. Cosolvent Effects on Protein Stability. *Annu. Rev. Phys. Chem.* **2013**, *64*, 273−293.
(32) van der Vegt, N. F. A.; Nayar, D. The Hydrophobic Effect and the Role of Cosolvents. *J. Phys. Chem. B* **2017**, *121*, 9986−9998.
(33) Nayar, D.; van der Vegt, N. F. A. Cosolvent Effects on Polymer Hydration Drive Hydrophobic Collapse. *J. Phys. Chem. B* **2018**, *122*, 3587−3595.
(34) Ma, J.; Straub, J. E.; Shakhnovich, E. I. Simulation study of the collapse of linear and ring homopolymers. *J. Chem. Phys.* **1995**, *103*, 2615−2624.
(35) Zangi, R.; Zhou, R.; Berne, B. J. Urea's Action on Hydrophobic Interactions. *J. Am. Chem. Soc.* **2009**, *131*, 1535−1541.
(36) Kavassalis, T. A.; Sundararajan, P. R. A Molecular Dynamics Study of Polyethylene Crystallization. *Macromolecules* **1993**, *26*, 4144−4150.
(37) Liao, Q.; Jin, X. Formation of segmental clusters during relaxation of a fully extended polyethylene chain at 300 K: A molecular dynamics simulation. *J. Chem. Phys.* **1999**, *110*, 8835−8841.
(38) Fujiwara, S.; Sato, T. Structure formation of a single polymer chain. I. Growth of trans domains. *J. Chem. Phys.* **2001**, *114*, 6455−6463.

(39) Tanaka, G.; Mattice, W. L. Chain collapse by atomistic simulation. *Macromolecules* **1995**, *28*, 1049−1059.
(40) Chudoba, R.; Heyda, J.; Dzubiella, J. Tuning the collapse transition of weakly charged polymers by ion-specific screening and adsorption. *Soft Matter* **2018**, *14*, 9631−9642.
(41) Okur, H. I.; Hladílková, J.; Rembert, K. B.; Cho, Y.; Heyda, J.; Dzubiella, J.; Cremer, P. S.; Jungwirth, P. Beyond the Hofmeister Series: Ion-Specific Effects on Proteins and Their Biological Functions. *J. Phys. Chem. B* **2017**, *121*, 1997−2014.
(42) Nayar, D.; Folberth, A.; van der Vegt, N. F. A. Molecular origin of urea driven hydrophobic polymer collapse and unfolding depending on side chain chemistry. *Phys. Chem. Chem. Phys.* **2017**, *19*, 18156−18161.
(43) Heyda, J.; Okur, H. I.; Hladílková, J.; Rembert, K. B.; Hunn, W.; Yang, T.; Dzubiella, J.; Jungwirth, P.; Cremer, P. S. Guanidinium can both Cause and Prevent the Hydrophobic Collapse of Biomacromolecules. *J. Am. Chem. Soc.* **2017**, *139*, 863−870.
(44) Rogers, B. A.; Okur, H. I.; Yan, C.; Yang, T.; Heyda, J.; Cremer, P. S. Weakly hydrated anions bind to polymers but not monomers in aqueous solutions. *Nat. Chem.* **2022**, *14*, 40−45.
(45) Thosar, A. U.; Patel, A. J. Hydration determines anion accumulation. *Nat. Chem.* **2022**, *14*, 8−10.
(46) Mukherjee, M.; Mondal, J. Osmolyte-Induced Collapse of a Charged Macromolecule. *J. Phys. Chem. B* **2019**, *123*, 4636−4644.
(47) Hess, B.; Kutzner, C.; van der Spoel, D.; Lindahl, E. GROMACS 4: Algorithms for Highly Efficient, Load-Balanced, and Scalable Molecular Simulation. *J. Chem. Theory Comput.* **2008**, *4*, 435−447.
(48) Tribello, G. A.; Bonomi, M.; Branduardi, D.; Camilloni, C.; Bussi, G. PLUMED 2: New Feathers for an Old Bird. *Comput. Phys. Commun.* **2014**, *185*, 604−613.
(49) Kumar, S.; Rosenberg, J. M.; Bouzida, D.; Swendsen, R. H.; Kollman, P. A. The Weighted Histogram Analysis Method for Free-Energy Calculations on Biomolecules. I. The method. *J. Comput. Chem.* **1992**, *13*, 1011−1021.
(50) Errington, J. R.; Debenedetti, P. G. Relationship between structural order and the anomalies of liquid water. *Nature* **2001**, *409*, 318−321.
(51) Chau, P.; Hardwick, A. J. A new order parameter for tetrahedral configurations. *Mol. Phys.* **1998**, *93*, 511−518.
(52) Athawale, M. V.; Goel, G.; Ghosh, T.; Truskett, T. M.; Garde, S. Effects of lengthscales and attractions on thecollapse of hydrophobic polymers in water. *Proc. Natl. Acad. Sci. U.S.A.* **2007**, *104*, 733−738.
(53) Chakrabarty, S.; Bagchi, B. Self-Organization of n-Alkane Chains in Water: Length Dependent Crossover from Helix and Toroid to Molten Globule. *J. Phys. Chem. B* **2009**, *113*, 8446−8448.
(54) Dzubiella, J. Salt-specific stability of short and charged alanine-based a-helices. *J. Phys. Chem. B* **2009**, *113*, 16689−16694.
(55) Monterroso, B.; Reija, B.; Jiménez, M.; Zorrilla, S.; Rivas, G. Charged molecules modulate the volume exclusion effects exerted by crowders on FtsZ polymerization. *PLoS One* **2016**, *11*, No. e0149060.

https://doi.org/10.1021/acspolymersau.4c00011
ACS Polym. Au 2024, 4, 289−301